Available online at www.sciencedirect.com
SCIENCE DIRECT®
Journal of Magnetic Resonance 164 (2003) 35–43
JMR Journal of Magnetic Resonance
www.elsevier.com/locate/jmr

Observation of echoes in reorientation processes of nematic liquid crystals

Michael Bender,[a,*] Peter Holstein,[b] and Dieter Geschke[a]

[a] *Fakultät für Physik und Geowissenschaften, Universität Leipzig, Linnéstraße 5, 04103 Leipzig, Germany*
[b] *SINUS Messtechnik GmbH, Föpplstraße 13, 04347 Leipzig, Germany*

Received 11 January 2003; accepted 2 June 2003

Abstract

Fast electrically driven reorientation processes of thermotropic nematic liquid crystals were investigated by means of ^{1}H NMR. The reorientation time is determined by the electric field and can be varied between several hundred milliseconds and less than 50 μs. Although the reorientation of the nematic director is limited to an angular range of 90°, echoes occur for reorientation times below 4 ms. It turned out that the separation of the sidebands is up to two orders of magnitude higher than it would be expected in MAS experiments. This behaviour can be understood in analogy to MAS by means of a time-dependent dipolar Hamiltonian; an exact description of the echo position is given for the heteronuclear dipolar interaction. The homogeneous sample rotation of the MAS experiment must be replaced by a more complex term which describes the director reorientation. Due to the non-linearity of this term, the separation of the sidebands is no longer proportional to the frequency of the sample rotation but can reach up to 20 times the maximum director frequency. The experimental results are presented together with a theoretical interpretation.

Keywords: Liquid crystal dynamics; Echoes; Sidebands; Time-dependent Hamiltonian; ^{1}H dipolar interaction

1. Introduction

The macroscopic reorientation of the NMR sample results in a time-dependent Hamiltonian. In most cases, the Hamiltonian can be separated in two terms A and T, where T describes the spin system and A describes the interaction with the lattice. Macroscopic motion affects A only while T remains unchanged. This has been widely exploited in MAS experiments [1–3] but is also true for other kinds of dynamic processes, such as mechanical flips of oriented smectic-A liquid crystals [4].

The reorientation process described in this work is the homogeneous director reorientation of thermotropic nematic liquid crystals (LCs). The reorientation of the LC molecules in external fields can be understood as the rotation of a macroscopic quantity which describes the mean orientation of the molecules in the sample and is called the director **n**. Due to the symmetric properties of most nematics there is no difference between **n** and −**n** and the reorientation is restricted to angles between 0° and 90°.

Another property of LCs is the anisotropy of the sample, which leads to broad solid-like ^{1}H NMR spectra for orientations parallel or perpendicular to the magnetic field and liquid-like ^{1}H NMR spectra with a well-resolved chemical shift in the proximity of the magic angle [5,6]. The reorientation process can be characterised as follows: (1) The sample is anisotropic and the spectra change significantly with the angle between $\mathbf{B}_0$ and **n**. (2) The angle between the rotational axis of the director and $\mathbf{B}_0$ is 90°. (3) The director reorientation is described by a non-periodic non-linear function with a well defined start and end point.

Even though this behaviour is quite different from the MAS experiment with a powder sample rotating uniformly under magic angle conditions, it can be described by the same formalism. One important difference has to be taken into account when the transformation from the MAS frame to the laboratory frame is carried out:

* Corresponding author.
E-mail addresses: bender@physik.uni-leipzig.de (M. Bender), hol@sinusmess.de (P. Holstein), geschke@physik.uni-leipzig.de (D. Geschke).

1090-7807/$ - see front matter © 2003 Elsevier Inc. All rights reserved.
doi:10.1016/S1090-7807(03)00189-7

the Euler angle $\alpha = \omega_{MAS}t$, describing the rotation of the MAS rotor in the probe, has to be replaced by a function $\varphi(t)$ which gives the time-dependent angle between the director and the magnetic field.

One noticeable consequence is a modification of the sideband separation. Due to the non-linearity of $\varphi(t)$ the separation is no longer determined by the frequency of the sample rotation but can increase up to significantly higher values. The experiments described here show sideband separations between several hundred hertz and 7 kHz for maximum director frequencies between 20 and 500 Hz. The sideband separation is therefore several times higher than the MAS sideband separation for rotor frequencies comparable to the maximum director frequency.

The investigation of such fast dynamic processes in LCs has been facilitated by the introduction of an electric field in addition to the magnetic field of the NMR spectrometer [6–8]. The director reorientation can be controlled in a very flexible way by the application of electric pulses of various shapes, voltages, and durations. The time-dependent angle between the director and the magnetic field is adjusted by the shape of the electric pulse and can be arbitrarily chosen, with the only restriction being that the director cannot be forced back into the direction of the magnetic field ($\Delta\varepsilon, \Delta\chi > 0$). Another advantage of electrically induced reorientation experiments is the possibility to vary the director frequency over several orders of magnitude by changing the applied voltage. Therefore, frequencies between a few hertz and several kilohertz can be investigated with similar accuracy. The analysis of the sideband separation enables the observation of the LC dynamics without disrupting the reorientation process. This is especially useful for fast processes which are otherwise difficult to investigate by NMR experiments.

2. Theory

The director reorientation leads to a time-dependent Hamiltonian which can be described with the same formalism as the sample rotation in MAS experiments. Like the first MAS experiments, only ^{1}H NMR spectra are available and we discuss therefore the rarely used case of the dipolar interaction [2,9]. The time-dependent Hamiltonian is derived together with an exact solution of the FID for the heteronuclear dipolar interaction. The echo position follows directly from this solution.

The time-dependent Hamiltonian can be derived by considering a single molecule with its long molecular axis aligned parallel to the director **n**. The director reorientation is controlled by the electric and magnetic field and is therefore restricted to the (E, B_0)-plane. The "rotor axis" $\boldsymbol{\Omega}$ of such a process is perpendicular to E, B_0, and n. The Hamiltonian in the laboratory frame (LAB) can be obtained by transformation from the principal axis system (PAS) of the interaction tensor to the director frame (DIR) and finally to the laboratory frame which is defined by the B_0 axis (see Fig. 1):

$$\mathrm{PAS} \overset{\phi,\theta,\psi}{\rightarrow} \mathrm{DIR} \overset{\alpha,\beta,\gamma}{\rightarrow} \mathrm{LAB}.$$

The director frame has been defined with the z-axis parallel to $\boldsymbol{\Omega}$, i.e., $\mathbf{e}_z^{\mathrm{DIR}} \| \boldsymbol{\Omega} \perp \mathbf{n}$. This type of rotational transformations can be performed with the Hamiltonian H expressed in terms of irreducible spherical tensors [10]:

$$H = C \cdot \sum_{k=0}^{2} \boldsymbol{A}^k \cdot \boldsymbol{T}^k = C \cdot \sum_{k=0}^{2} \sum_{q=-k}^{+k} (-1)^q A_q^k T_{-q}^k. \tag{1}$$

The Hamiltonian separates into a term $\boldsymbol{A}^k$ which describes the interaction with the lattice and in a second term $\boldsymbol{T}^k$ which describes the spin system. The director dynamics affects only $\boldsymbol{A}^k$ and leaves $\boldsymbol{T}^k$ unchanged. It is therefore sufficient to find $\boldsymbol{A}^{k\,\mathrm{LAB}}$ in the laboratory system. This has been done in Appendix A. The result with no restrictions to the angles α and β is given by Eq. (A.4). However, as shown in Fig. 1, the director reorientation is restricted to the (E, B_0) plane with its "rotor axis" $\boldsymbol{\Omega}$ perpendicular to B_0 and β is therefore 90°. The Euler angle α describes the rotation about the z-axis of the director frame and has to be replaced by the time-dependent angle $\varphi(t)$ between the director and the magnetic field B_0. In this case, Eq. (A.4) simplifies considerably:

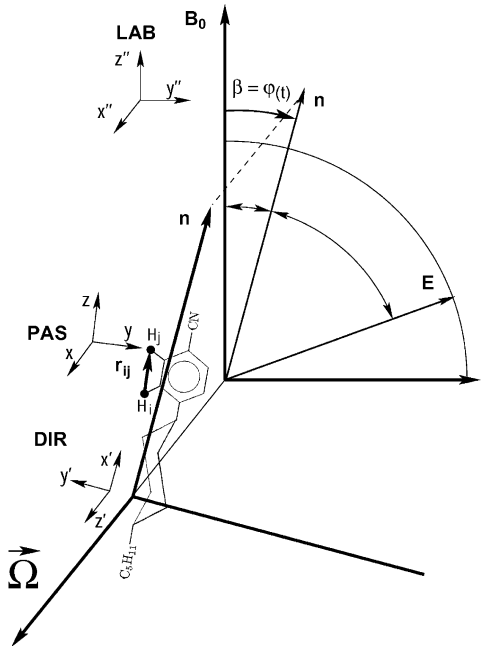

Fig. 1. Frames of reference: The director reorientation is equivalent to the rotation of a rotor with its axis $\boldsymbol{\Omega}$ perpendicular to the magnetic field and the molecules oriented along an axis **n** perpendicular to the rotor axis.

$$A_0^{(2)\,\mathrm{LAB}} = A_0^{(2)\,\mathrm{PAS}}\left[\frac{3}{4}\sin^2\theta\cos(2\varphi(t)+2\psi) + \frac{1}{4}(3\cos^2\theta-1)\right]. \quad (2)$$

The angle $\varphi(t)$ in a homogeneous director reorientation of a nematic liquid crystal in static external fields can be described [6,11] by:

$$\varphi(t) = \arctan\left\{\tan(\varphi_0-\varphi_{\mathrm{es}})\exp\left(-\frac{t}{\tau}\right)\right\}+\varphi_{\mathrm{es}}, \quad (3)$$

where φ_0 is the initial angle between n and B_0 for $t=0$, φ_{es} is the equilibrium position where the reorientation ends ($t \gg \tau$), and τ is the time constant which characterises the dynamic process. The experiments described here always start with the director aligned parallel to the magnetic field, i.e., $\varphi_0 = 0$. The equilibrium φ_{es} depends on the competing torques of the electric and magnetic field and therefore on the strength of both fields and the angle between them.

With the results of Appendix A the representation of the dipolar Hamiltonian in the laboratory frame is known and the evolution of the system can be described. The time evolution of the density matrix ϱ is described by the von Neumann equation with the formal solution:

$$\varrho(t) = U(t)\varrho(0)U^{-1}(t). \quad (4)$$

The propagator $U(t)$ of a Hamiltonian which is not explicitly time-dependent ($\partial H/\partial t = 0$) is of the form:

$$U(t) = \mathrm{e}^{-\mathrm{i}Ht}. \quad (5)$$

The term Ht has to be replaced by an integral $\int H(t')\mathrm{d}t'$ if the Hamiltonian changes in time. The NMR experiments described in this work can already be understood by a simple $\pi/2$ experiment: the initial state $\varrho(0)$ is therefore given by $\mathbf{I}_x$, assuming a $(\pi/2)_x$-pulse. The time evolution [Eq. (4)] can be written as:

$$\varrho(t) = \exp\left(\int_{t_1}^{t_1+t} H(t')\,\mathrm{d}t'\right)\varrho(0)\exp\left(-\int_{t_1}^{t_1+t} H(t')\,\mathrm{d}t'\right). \quad (6)$$

The time axes of $H(t)$ and $\varrho(t)$ are different. The Hamiltonian as derived in Eqs. (A.5) and (A.6) depends on $\varphi(t)$, i.e., a time axis which is defined by the reorientation process. The time axis of the FID starts with the $\pi/2$ pulse and is shifted by t_1 relative to the reorientation process (see Fig. 2). The integral $\int_0^t H(t')\mathrm{d}t'$ has therefore to be replaced by $\int_{t_1}^{t_1+t} H(t')\mathrm{d}t'$ in order to evaluate the Hamiltonian at the correct time.

Eq. (6) can be solved for a time-independent Hamiltonian and leads for the heteronuclear dipolar interaction to the time signal:

$$M_x(t) \sim \cos(\omega_{\mathrm{IS}}t) \quad (7)$$

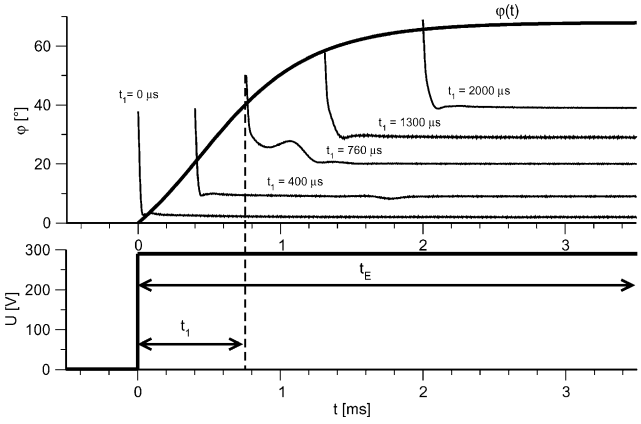

Fig. 2. Basic LC reorientation experiment with an electric pulse (bottom) of variable duration t_{E} which starts the director reorientation. The angle $\varphi(t)$ between $\mathbf{n}$ and B_0 (top) is shown with ^{1}H NMR FIDs taken with different delays t_1 for a process with $\tau = 438\,\mu\mathrm{s}$ (top). The FIDs with $t_1 = 0\cdots400\cdots760\cdots1310\cdots2000\,\mu\mathrm{s}$ are taken from Fig. 4.

with the transition frequency:

$$\omega_{\mathrm{IS}} = \frac{\mu_0\hbar}{4\pi}\gamma_{\mathrm{I}}\gamma_{\mathrm{S}}\sqrt{\frac{2}{3}}A_0^{(2)\,\mathrm{LAB}}. \quad (8)$$

A solution for the homonuclear dipolar interaction does not exist, due to the multi-particle character of the Hamiltonian. The Hamiltonians $H(t)$ do not commute for all times and the integrals in Eq. (6) cannot be evaluated. However, there are approximations [9,12] which also lead to a cosine-law and give comparable results.

The time signal [Eq. (7)] can be obtained from Eq. (8) with $A_0^{(2)\,\mathrm{LAB}}$ replaced by Eqs. (A.4) or (2). In the time-dependent case, the product $\omega_{\mathrm{IS}}t$ has to be replaced by the integral $\int\omega_{\mathrm{IS}}(t')\mathrm{d}t'$. This integral can be solved as shown in Appendix B. In case of the director reorientation ($\beta = 90°$) the argument of the cosine is given by Eq. (B.10); with $I_2(t)$ replaced by Eq. (B.7), the time signal has the form:

$$M_x(t) \sim \cos\left(\int_{t_1}^{t_1+t}\omega_{\mathrm{IS}}(t')\,\mathrm{d}t'\right) \sim \cos\left(\frac{\mu_0\hbar}{4\pi}\frac{\gamma_{\mathrm{I}}\gamma_{\mathrm{S}}}{r_{ij}^3}\cdot f(t)\right) \quad (9)$$

with

$$\begin{aligned} f(t) = {} & \left(\frac{1}{4}+\frac{3}{4}\cos(2\varphi_{\mathrm{es}})\right)t+\frac{3}{4}\cos(2\varphi_{\mathrm{es}})\tau \\ & \times\left(\ln\left\{1+\tan^2(-\varphi_{\mathrm{es}})\exp\left(-\frac{2(t_1+t)}{\tau}\right)\right\}\right. \\ & \left.-\ln\left\{1+\tan^2(-\varphi_{\mathrm{es}})\exp\left(-\frac{2t_1}{\tau}\right)\right\}\right) \\ & +\frac{3}{4}\sin(2\varphi_{\mathrm{es}})2\tau\left(\arctan\left\{\tan(-\varphi_{\mathrm{es}})\exp\left(-\frac{t_1+t}{\tau}\right)\right\}\right. \\ & \left.-\arctan\left\{\tan(-\varphi_{\mathrm{es}})\exp\left(-\frac{t_1}{\tau}\right)\right\}\right). \end{aligned} \quad (10)$$

It is obvious that the time signal depends not only on the parameters φ_0, φ_{es}, and τ of the reorientation process

but also on the delay t_1 between the beginning of the reorientation process and the start of the NMR experiment. It is therefore possible to obtain different echo positions or sideband separations from the same dynamic process by changing the delay t_1.

An echo occurs at times where the state $\varrho(t)$ becomes equal to the initial state $\varrho(0)$. Regarding Eq. (9) this is the case where the argument of the cosine $\int_{t_1}^{t_1+t} H(t')\mathrm{d}t'$ vanishes ($f(t) = 0$). Roots of Eq. (10) exist between $\varphi(t = 0) = 0$ and $\varphi(t_{\mathrm{MAG}}) = 54.7°$, i.e., in the interval $[0, t_{\mathrm{MAG}}]$ with the magic angle passage of the director at:

$$t_{\mathrm{MAG}} = -\tau \ln\left(\frac{\tan(54.7° - \varphi_{\mathrm{es}})}{\tan(-\varphi_{\mathrm{es}})}\right). \tag{11}$$

The echo maximum shifts therefore to the beginning of the FID as t_1 increases. At $t_1 = t_{\mathrm{MAG}}$ the echo coincides with the FID itself and for times $t_1 > t_{\mathrm{MAG}}$ no echo exists. As a consequence the sideband separation which is given by $1/t_{\mathrm{echo}}$ approaches infinity as $t_{\mathrm{echo}} \to 0$.

So far only one isolated spin pair with an internuclear vector $\mathbf{r}_{ij}$ has been considered. The molecules in nematic liquid crystals are oriented along a preferred axis which defines the director **n**. The orientational order is described by a distribution function $f(\theta, \psi)$ which gives the probability of finding a molecule with its long molecular axis in an orientation (θ, ψ) with respect to the director. The NMR spectrum is determined by the average of all molecular orientations. This process can technically be described by averaging over (θ', ψ') during the transformation from the molecular system (MOL) to the director system (DIR). One more transformation has therefore to be added between the PAS and the LAB:

$$\mathrm{PAS} \overset{\eta,\xi,\zeta}{\to} \mathrm{MOL} \overset{\phi',\theta',\psi'}{\to} \mathrm{DIR} \overset{\alpha,\beta,\gamma}{\to} \mathrm{LAB}.$$

Using the same formalism as above results in:

$$V_0^{(2)\mathrm{LAB}} = \sum_{q=-2}^{+2} \times \sum_{q'=-2}^{+2} V_0^{(2)\mathrm{PAS}} d_{0q'}^{(2)}(\xi)\, \mathrm{e}^{\mathrm{i}\zeta q'} \langle \mathrm{e}^{\mathrm{i}\phi' q'} d_{q'q}^{(2)}(\theta') \rangle\, \mathrm{e}^{\mathrm{i}\alpha q} d_{q0}^{(2)}(\beta). \tag{12}$$

The angles γ and ϕ' have been dropped for the same reasons as in Eq. (A.3) and η can arbitrarily be chosen for uniaxial liquid crystals. Eq. (12) is of the same type as Eq. (A.3). The quantities $\langle \mathrm{e}^{\mathrm{i}\phi' q'} d_{q'q}^{(2)}(\theta') \rangle$ are related to the Mayer–Saupe order matrix [13]. The above results can therefore be applied to liquid crystals, provided that the scaling of the dipolar interaction by the order parameters is taken into account. In particular, the sideband separation is independent of the distribution function and represents a general feature of this reorientation process.

The LCs investigated in this work can be described as uniaxial rodlike LCs. In this case, only the diagonal elements of the order matrix have to be taken into account and due to the complete cylindrical symmetry, only one scalar order parameter S remains. The angles (θ, ψ) in Eq. (A.4) have therefore to be set to $\theta = 90°$ and $\psi = 0°$.

3. Experimental

The ^{1}H NMR experiments were carried out on a Bruker MSL 100 spectrometer working with a 2.35-T magnetic field at 100 MHz. The probe used was a laboratory-made single-channel ^{1}H/^{19}F probe designed for high voltage experiments. A goniometer facility allows a very precise setting of the angle between the sample and the B_0 field. A single $\pi/2$ pulse with a duration of 2 μs was used in all experiments. The FID was recorded with a dwell time of 3 μs and 2048 data points. The spectra were analysed with the Gifa NMR processing software [14].

The director reorientation of the nematic liquid crystals is controlled by an additional experimental setup which is connected to the NMR spectrometer. Initially, the director aligns parallel to the magnetic field but the application of electric fields perpendicular ($\Delta\varepsilon, \Delta\chi > 0$) to the spectrometer field allows reorientation experiments in the range between 0° and 90° with respect to B_0. High voltage pulses on thin capacitor samples provide electric fields up to several MVm^{-1}. These samples are filled with the LC under investigation and placed in the 8 mm NMR coil of the probe. A computer-controlled setup based on a programmable function generator and a high voltage amplifier provides high voltage pulses up to 1000 V. Shape, duration, and voltage can be chosen as required. The duration of the pulses is limited only by the rise time of approx. 10 μs.

The LC switching experiment is synchronised with the NMR spectrometer. The combination of NMR experiments and LC switching makes it possible to set the voltage and duration of the electric pulses within the NMR pulse program and therefore to change the state of the sample during the course of the NMR pulse sequence. A detailed description of the experimental setup and the design of the LC cells can be found elsewhere [6,7,15].

The low-molar-mass thermotropic LC used is the well-known 4-(*trans*-4-pentylcyclohexyl)benzonitrile (PCH-5) [16,17]. This LC is particularly suitable for fast switching experiments in electric fields because of its high dielectric anisotropy ($\Delta\varepsilon = 12.7$, $\gamma_1 = 0.1337$ Pas at 22.1 °C) and its small rotational viscosity. The LC is filled in a 150-μm capacitor cell. At room temperature, reorientation times between $\tau = 4.4$ ms and $\tau = 40$ μs could be achieved with high voltage pulses between 100 and 1000 V, i.e., electric fields between 0.67 and $6.7\,\mathrm{MVm}^{-1}$. The angle between E and B_0 has been

chosen as 70° for all experiments. An angle close to 90° would provide a larger angular range but because τ increases with this angle considerably higher voltages would have been required.

The basic experiment is described in Fig. 2. The director reorientation is started by a square pulse of duration t_E. The time constant τ [Eq. (3)] of the reorientation process depends on the applied voltage, the angle between the electric and magnetic field and some material properties [11,15] and decreases with increasing voltage. After a delay t_1 from the beginning of the electric pulse, the $\pi/2$ pulse is applied to the sample and the FID is taken.

This basic experiment can be varied in several ways. One option is to investigate the director orientation after the application of an electric pulse of duration t_E. The $\pi/2$ pulse is applied after the electric pulse and, provided that the reorientation back into the magnetic field of the spectrometer can be neglected, the FID represents the static orientation of the sample at the time $t_1 = t_E$. The different intermediate states of the dynamic process can be investigated with this kind of experiment by changing the duration t_E of the electric pulse. The time constant τ can be determined in this way [7,15]. τ is an important parameter in Eq. (10) and has therefore been measured independently with such an experiment. Each reorientation process with a given τ (or given voltage) was sampled using a series of t_E values in the range of $t_E = 0, \ldots, 5\tau$. Furthermore, the analysis of these spectra provides the information if the reorientation process is homogeneous. Eq. (3) is only valid in this case [18]. Another type of experiment can be carried out if the $\pi/2$ pulse is started while the electric field is still applied to the sample ($t_1 < t_E$). In this case, the director reorientation continues during the data acquisition and the FID represents the macroscopic dynamics of the sample. Square pulses with a duration $t_E > t_1 + DW \cdot N_D$, where N_D is the number of data points and DW is the dwell time, were used in order to guarantee that the dynamics during the data acquisition can be described by Eq. (3). One advantage of this experiment is that the dynamic process can be investigated without being disturbed as in the above case. Different parts of the reorientation process were investigated by changing the delay t_1.

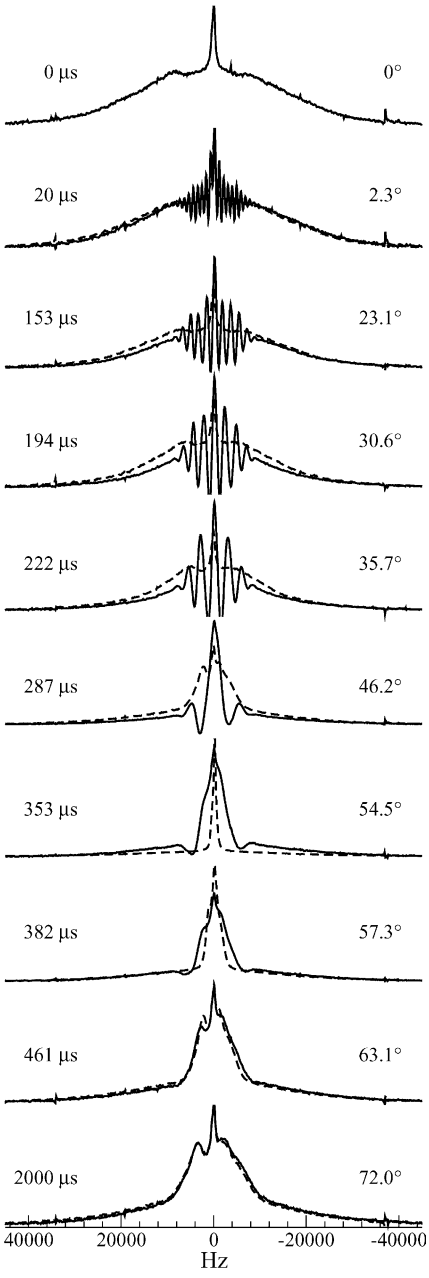

Fig. 3. ^{1}H NMR spectra of PCH-5 taken in different orientations. The start of the NMR experiment (t_1) relative to the reorientation experiment is given on the left side of the spectra, the angle between $\mathbf{n}$ and $\mathbf{B}_0$ at t_1 on the right side. The spectra taken in a static state (dashed line) are shown together with the spectra obtained while the reorientation process is in progress (solid line). The first spectrum is a static spectrum of PCH-5 with $\mathbf{n} \| \mathbf{B}_0$.

4. Results

A number of reorientation processes of PCH-5 with time constants τ varying from 4.4 ms down to 104 μs were investigated. For every given value of τ, 30 spectra were taken and analysed. Fig. 3 shows some selected ^{1}H NMR spectra of a reorientation process with $\tau = 155$ μs. The top spectrum was taken with the director aligned parallel to the B_0 field ($E = 0$). The spectral width changes during the director reorientation according to the second Legendre polynomial $P_2(\cos\varphi)$ (dashed lines in Fig. 3). They were taken with $t_E = t_1$, i.e., with the director frozen at the specified angle. The minimum linewidth is obtained near the magic angle (Fig. 3, $t_1 = 353$ μs) where the dipolar interaction is nearly completely averaged out and ^{1}H chemical shift patterns appear [6]. These spectra were used to obtain the time constant τ.

The second set of spectra in Fig. 3 (solid lines) was taken while the electric reorientation was in progress ($t_E > 5\tau$) and shows pronounced sidebands. It can be seen that the sideband separation increases significantly with t_1 and that no sidebands can be found for $\varphi > 54.7°$. The central peak in the first spectra and the broad wings in the last spectra are due to the epoxy resin which was used to seal the LC cells. This component does not take part in the reorientation and can be ignored. However, it is possible to remove these components by special background suppression techniques [7].

Sidebands in the spectra are equivalent to echoes in the FIDs. The echo position t_{echo} depends on the time constant τ of the reorientation process and the delay t_1 between the start of the reorientation experiment and the beginning of the FID. The acquisition of the FIDs relative to the electric pulse and the director reorientation $\varphi(t)$ is indicated in Fig. 2. As an example, five FIDs with different delays t_1 are plotted together with the time-dependent angle $\varphi(t)$ between the director n and B_0. Fig. 4a and d show the FIDs of two complete reorientation processes, where τ is constant (a) $\tau = 438\,\mu s$ (294 V), (b) $\tau = 155\,\mu s$ (498.5 V)) while t_1 increases from bottom to top. The echo position shifts to the beginning of the FID as τ decreases or t_1 increases. First echoes could be found in a process with $\tau = 4.44$ and $t_1 = 7.68\,ms$ at 3.5 ms. This is large compared with the spin–spin relaxation T_2 of approx. 200 μs. The insert of Fig. 4a shows a series of FIDs taken with $t_E = t_1$ while all other experimental conditions were unchanged.

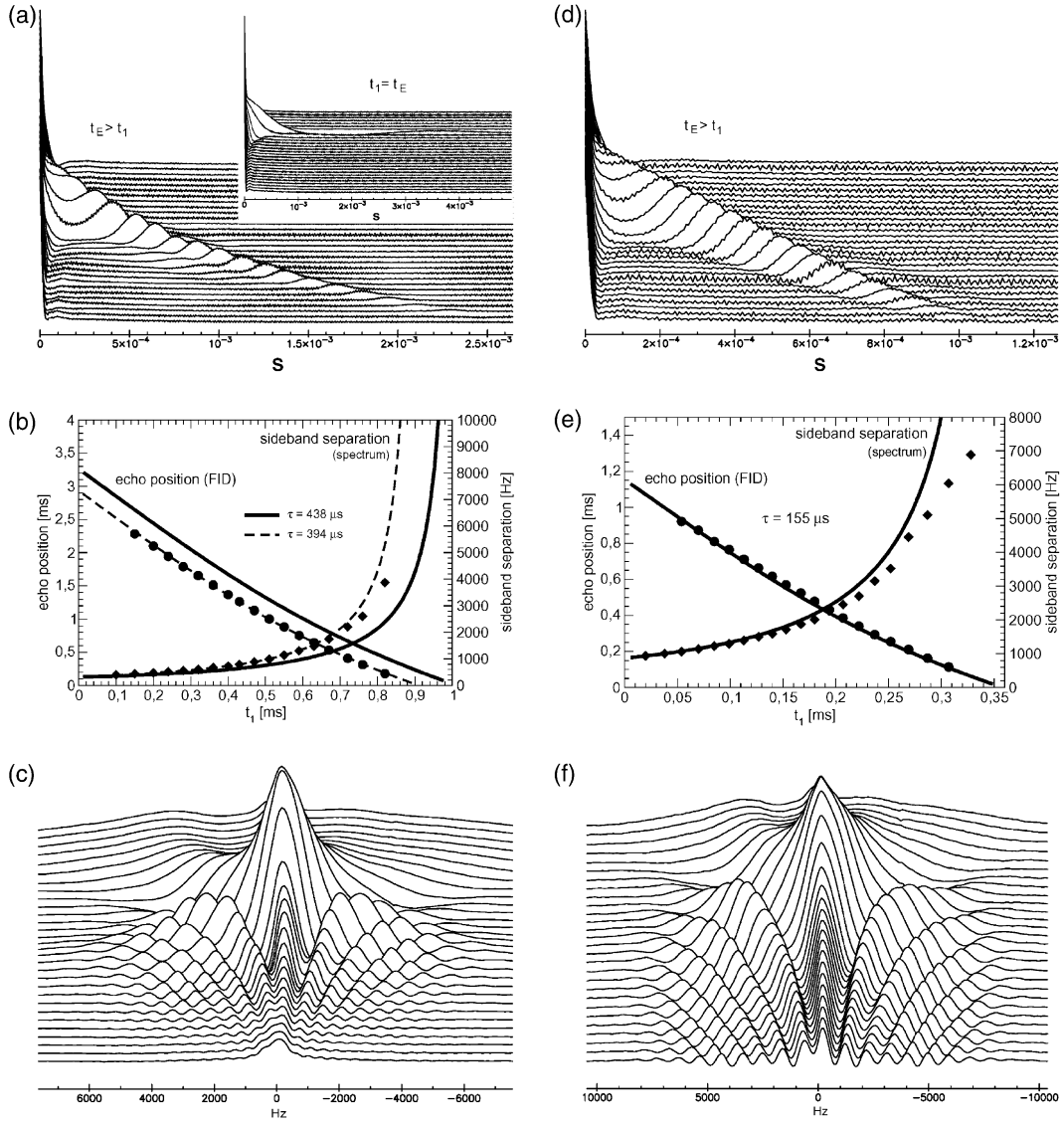

Fig. 4. ^{1}H NMR FIDs (top) and spectra (bottom) of PCH-5 for two different time constants: $\tau = 438\,\mu s$ (a–c), $\tau = 155\,\mu s$ (d–f). In the plots (b) and (e), the echo position and sideband separation is shown together with the theoretical predictions according to Eq. (9). The experimental echo position (●) and sideband separation (◆) is shown in (b) and (e) and can be compared with the theoretical predictions (solid and dashed lines).

In these static situations, no echoes appear, but T_2 increases as the director draws near to the magic angle. The decay of the magnetisation can be observed over more than 4 ms in the vicinity of 54.7°. The spectra (Fig. 4c and f) show equally spaced sidebands. The number of sidebands decreases with decreasing t_{echo} while the sideband separation increases. The frequency range in Fig. 4c and f has been chosen to visualise the sideband separation. An example of the full spectra was given in Fig. 3 which is a subset of Fig. 4f. The echo position t_{echo} (●) and the sideband separation (◆) as a function of t_1 are shown in Fig. 4b and e.

The distortions in the FIDs and spikes in the spectra are caused by the wires connected to the capacitor cell. These wires form a closed circuit through the NMR coil which transfers noise from the surroundings to the receiver of the NMR spectrometer [5,19].

The development of the sideband separation as a function of t_1 is by no means related to the frequency of the director reorientation. The director frequency $\nu(t)$ shows a maximum at $\nu_{\max} = (4\pi\tau)^{-1}$ and decreases for

$$t > t_{\max} = \frac{\tau}{2}\ln(\tan^2(\varphi_0 - \varphi_{\text{es}})) \tag{13}$$

while the sideband separation increases continuously until the magic angle has been reached (see Eq. (11)). Furthermore, the sideband separation is higher than the director frequency. Values of $\sim 3\nu_{\max}$ have been found for short delays t_1 which increase up to $\sim 20\nu_{\max}$ for $t_1 \approx \tau$.

The results of the theoretical section [Eq. (9)] are needed to describe the echo position. Even though these results have been obtained by treating a heteronuclear two-spin-system they can be applied to the experimental data of a homonuclear multi-spin-system. As shown in Fig. 4b and e the experimental data are close to the values predicted by the theory (solid line, left scale). The graph was computed numerically from the roots of Eq. (10) for different values of t_1. Theory and experiment match almost ideally for the 155 μs process (Fig. 4e). In the other case (Fig. 4b), the best conformity with the experiment could be found for $\tau = 394\,\mu\text{s}$ (dashed line) which is somewhat faster than the result of the static experiments ($t_{\text{E}} = t_1$) leading to $\tau = 438\,\mu\text{s}$ (solid line). Nevertheless, both results agree within the margins of the experimental error which is about 5% in static experiments with long electric pulses [15]. In the case of short pulses, the rising time and imperfect pulse shapes lead to errors above 10%. The shape of the graph is in all cases ($155\,\mu\text{s} \leqslant \tau \leqslant 4.4\,\text{ms}$) nearly identical to the experimental data even though the τ data differ in some cases slightly from the static results. There are no indications for multiple echoes in the FIDs, which also supports the theory. The sideband separation can be computed from the echo position: the sidebands can be found at $1/t_{\text{echo}}$. The measured sideband separation and the calculated $1/t_{\text{echo}}$ values can also be found in Fig. 4b and e, right scale.

The fit to the measured sideband separation is less accurate for large delays t_1 in particular. This is caused by the echo which moves to the beginning of the FID as t_1 increases. According to the theory, t_{echo} becomes zero as the magic angle is reached. Sidebands with a separation tending to infinity would follow but cannot be seen for experimental reasons: for t_1 close to the magic angle passage (see Eq. (11)), the echo maximum is located at the beginning of the FID and therefore cannot be well resolved. This leads to a line-broadening near the magic angle, where only one weak pair of sidebands can be identified.

5. Conclusion

It was possible to investigate echoes and sidebands in fast non-periodic director reorientations. The time-dependent Hamiltonian and a theoretical description of the non-linear dynamic process was given. The echo position was calculated and experimentally verified also. The effect of sample anisotropy is described and the theoretical predictions are in good agreement with the experimental results.

This work describes the effect of the director reorientation on the spectrum which is not only useful for investigating dynamic processes without disrupting them but is also important for estimating its influence in "static" situations where slow reorientation processes cannot always be avoided. The results already provide a new technique for measuring the time constant τ which is particularly useful in high magnetic fields where the reorientation back in the magnetic field is too fast to allow static experiments in different orientations to be performed. These techniques could also be applied to non-liquid-crystalline materials using molecules dissolved in liquid crystalline solvents. Furthermore, the nematic reorientation in electric and magnetic fields provides a model system for a well-known non-linear dynamic process which may be useful beyond LC research.

In this work, only the dipolar interaction has been considered. Extension of the theory to other interactions, e.g., the chemical shift or quadrupolar interaction, should lead to comparable results. In case of the chemical shift, a discussion of the spectral shape should be possible and would lead to more detailed results. It might also be possible to combine the manipulation of the spatial part of the Hamiltonian with pulse groups which act on the spin part.

Acknowledgments

The Deutsche Forschungsgemeinschaft (DFG) is acknowledged for financial support (HO 1619/5-1,3) and

E. Merck, Darmstadt (Germany) for providing the liquid crystals.

Appendix A

The dipolar Hamiltonian in a rotating frame of reference (see Fig. 1) can be described in terms of irreducible spherical tensors. The transformation into a system which rotates with the director (DIR) can be expressed by the Wigner rotation matrices $D^{(2)}_{qq'}$:

$$A_0^{(2)\,\mathrm{LAB}} = \sum_{q'}\sum_{q''} A_{q''}^{(2)\,\mathrm{PAS}} D^{(2)}_{q''q'}(\phi\theta\psi) D^{(2)}_{q'0}(\alpha\beta\gamma), \tag{A.1}$$

together with the reduced rotation matrices $d^{(2)}_{qq'}(\lambda)$ [10,20]:

$$D^{(2)}_{qq'}(\delta\lambda\sigma) = \mathrm{e}^{\mathrm{i}\delta q} d^{(2)}_{qq'}(\lambda)\ \mathrm{e}^{\mathrm{i}\sigma q'}. \tag{A.2}$$

The Euler angles (α,β,γ) and (ϕ,θ,ψ) as defined by Rose [21] specify the rotations. The angle γ can arbitrarily be chosen as 0° because all interactions are invariant to rotations about the B_0 axis. In case of the dipolar interaction, this is also true for the angle ϕ which performs a rotation about the internuclear vector $\mathbf{r}_{ij}$. Considering $A_0^{(2)\,\mathrm{PAS}} = \sqrt{\frac{3}{2}} r_{ij}^{-3}$ and $A_{\pm1}^{(2)\,\mathrm{PAS}} = A_{\pm2}^{(2)\,\mathrm{PAS}} = 0$ for the dipolar interaction, Eq. (A.1) simplifies to:

$$A_0^{(2)\,\mathrm{LAB}} = A_0^{(2)\,\mathrm{PAS}} \sum_{q'} \mathrm{e}^{-\mathrm{i}q'(\alpha+\psi)}\ d^{(2)}_{0q'}(\theta)\ d^{(2)}_{q'0}(\beta). \tag{A.3}$$

The reduced rotation matrices $d^{(2)}_{qq'}(\lambda)$ provide the angle-dependent irreducible spherical tensor $A_0^{(2)\,\mathrm{LAB}}$ [9]:

$$\begin{aligned} A_0^{(2)\,\mathrm{LAB}} = A_0^{(2)\,\mathrm{PAS}} \Bigg[& \frac{3}{4}\sin^2\beta\sin^2\theta\cos(2\alpha+2\psi) \\ & -\frac{3}{4}\sin 2\beta\sin 2\theta\cdot\cos(\alpha+\psi) \\ & +\frac{1}{4}(3\cos^2\beta-1)(3\cos^2\theta-1)\Bigg]. \end{aligned} \tag{A.4}$$

This result simplifies in case of the director reorientation (Eq. (2)).

Considering that only tensors of rank 2 contribute to the Hamiltonian, it can be obtained from Eq. (1) using the appropriate values for C and $T_0^{(2)}$:

$$H^{\mathrm{IS}} = C T_0^{(2)} A_0^{(2)\,\mathrm{LAB}} = -\sqrt{\frac{8}{3}}\frac{\mu_0}{4\pi}\gamma_{\mathrm{I}}\gamma_{\mathrm{S}}\hbar^2 I_{zi} S_{zj} A_0^{(2)\,\mathrm{LAB}} \tag{A.5}$$

in the case of heteronuclear dipolar interaction and:

$$H^{II} = -\sqrt{\frac{2}{3}}\frac{\mu_0}{4\pi}\gamma^2\hbar^2\left(3I_{zi}I_{zj} - \boldsymbol{I}_i\boldsymbol{I}_j\right) A_0^{(2)\,\mathrm{LAB}} \tag{A.6}$$

in the case of homonuclear interaction. $A_0^{(2)\,\mathrm{LAB}}$ is given by Eqs. (A.4) or (2).

Appendix B

The time signal of a reorienting nematic liquid crystal depends on the integral:

$$\int_{t_1}^{t_1+t} \omega(t')\,\mathrm{d}t', \tag{B.1}$$

where the transition frequency is given by Eqs. (8) and (A.4). Neglecting constant factors the integral:

$$\int\left(\frac{3}{4}A\cos\left(2\psi+2\varphi(t')\right) - \frac{3}{4}B\cos\left(\psi+\varphi(t')\right) + \frac{1}{4}C\right)\mathrm{d}t', \tag{B.2}$$

with

$$A = \sin^2\beta\sin^2\theta, \tag{B.3}$$

$$B = \sin 2\beta\sin 2\theta, \tag{B.4}$$

$$C = (3\cos^2\beta-1)(3\cos^2\theta-1), \tag{B.5}$$

and $\varphi(t)$ given by Eq. (3) has to be solved. The integrals $\int\cos(2\alpha+2\varphi(t'))\,\mathrm{d}t'$ and $\int\cos(\alpha+\varphi(t'))\,\mathrm{d}t'$ can be directly evaluated by means of the trigonometric identities and standard techniques:

$$\begin{aligned} I_1(t) &= \int\cos\Big(2(\psi+\varphi_{\mathrm{es}}) \\ &\qquad + 2\arctan\left\{F\mathrm{e}^{-t'/\tau}\right\}\Big)\mathrm{d}t' \\ &= D\left[t+\tau\ln\left(1+F^2\mathrm{e}^{-(2t)/\tau}\right)\right] \\ &\quad + E2\tau\ \arctan\left(F\mathrm{e}^{-t/\tau}\right) \end{aligned} \tag{B.6}$$

and

$$\begin{aligned} I_2(t) &= \int\cos\left(\psi+\varphi_{\mathrm{es}}+\arctan\left\{F\mathrm{e}^{-t'/\tau}\right\}\right)\mathrm{d}t' \\ &= G\tau\,\mathrm{arctanh}\left[\left(1+F^2\mathrm{e}^{-(2t)/\tau}\right)^{-(1/2)}\right] \\ &\quad + H\tau\ln\left[F\mathrm{e}^{-t/\tau}+\left(1+F^2\mathrm{e}^{-(2t)/\tau}\right)^{-(1/2)}\right] \end{aligned} \tag{B.7}$$

with

$$\begin{aligned} &D = \cos(\psi+\varphi_{\mathrm{es}}), \quad G = \cos(2\psi+2\varphi_{\mathrm{es}}), \\ &E = \sin(\psi+\varphi_{\mathrm{es}}), \quad H = \sin(2\psi+2\varphi_{\mathrm{es}}), \\ &F = \tan(\varphi_0-\varphi_{\mathrm{es}}). \end{aligned} \tag{B.8}$$

Combining all the above provides:

$$\begin{aligned} \int_{t_1}^{t_1+t}\omega(t')\,\mathrm{d}t' = C_{\mathrm{D}}\Bigg(&\frac{3}{4}A\big(I_2(t_1+t)-I_2(t_1)\big) \\ &-\frac{3}{4}B\Big(I_1(t_1+t)-I_2(t_1)\Big)+\frac{1}{4}Ct\Bigg). \end{aligned} \tag{B.9}$$

The experiments described in this work are characterised by $\beta=\theta=90°$ ($A=C=1$, $B=0$), $\psi=0°$ and $\varphi_0=0°$ which leads to a simplified result:

$$\int_{t_1}^{t_1+t} \omega(t')\,\mathrm{d}t' = C_\mathrm{D}\left(\frac{3}{4}(I_1(t_1+t)-I_1(t_1))+\frac{1}{4}t\right), \tag{B.10}$$

where C_D is given by:

$$C_\mathrm{D} = \frac{\mu_0\hbar}{4\pi}\frac{\gamma_I\gamma_S}{r_{ij}^3}. \tag{B.11}$$

Except for the constant factor C_D, this solution is identical to $f(t)$ in Eq. (10) and has been used to compute the echo position.

References

[1] M.M. Maricq, J.S. Waugh, NMR in rotating solids, J. Chem. Phys. 70 (7) (1979) 3300–3316.

[2] E.R. Andrew, The narrowing of N.M.R. spectra of solids by high-speed specimen rotation and the resolution of chemical shift and spin multiplet structures for solids, Part 1 of Progress in Nuclear Magnetic Resonance Spectroscopy, vol. 8, first ed., Pergamon Press, Oxford, New York, 1971, pp. 1–38.

[3] E.R. Andrew, Magic angle spinning, in: D.M. Grant, R.K. Harris (Eds.), Encyclopedia of NMR, vol. 5, Wiley, Chichester, New York, 1996, pp. 2891–2901.

[4] H. Schmiedel, B. Hillner, S. Grande, NMR magic echo in liquid crystals by sample reorientation, Phys. Lett. A 78 (5 and 6) (1980) 458–459.

[5] P. Holstein, A.C.D. Lopes, J. Rauchfuß, D. Geschke, ^{1}H multiple-pulse solid-state NMR investigations of electrically oriented liquid crystals, Magn. Reson. Chem. 35 (1997) 420–423.

[6] M. Bender, P. Holstein, D. Geschke, Electrically induced dynamic processes in nematic liquid crystals: ^{1}H nuclear magnetic resonance investigations, J. Chem. Phys. 113 (6) (2000) 2430–2439.

[7] M. Bender, Untersuchung elektrisch induzierter dynamischer Prozesse in Flüssigkristallen mit Hilfe der NMR, Ph.D. thesis, Universität Leipzig, Available from <http://dol.uni-leipzig.de/pub/2001-45>, 2001.

[8] C.J. Dunn, G.R. Luckhurst, T. Miyamoto, H. Naito, A. Sugimura, B.A. Timimi, A deuterium nuclear magnetic resonance investigation of field induced director dynamics in a nematic slab subject to magnetic and pulsed electric fields, Mol. Cryst. Liq. Cryst. 347 (2000) 167–178.

[9] I.J. Lowe, Free induction decays of rotating solids, Phys. Rev. Lett. 2 (7) (1959) 285–287.

[10] M. Mehring, Principles of High Resolution NMR in Solids, second ed., Springer, Berlin, 1983.

[11] P.G. de Gennes, J. Prost, The Physics of Liquid Crystals, second ed., Clarendon, Oxford, 1993.

[12] I.J. Lowe, R.E. Norberg, Free-induction decays in solids, Phys. Rev. 107 (1) (1957) 46–61.

[13] R.Y. Dong, Nuclear Magnetic Resonance of Liquid Crystals, Springer, New York, 1994.

[14] J.L. Pons, T.E. Malliavin, M.A. Delsuc, Gifa v4: a complete package for NMR dataset processing, J. Biomol. NMR 8 (1996) 445–452.

[15] M. Bender, P. Holstein, D. Geschke, Nematic reorientation in electric and magnetic fields, Liq. Cryst. 28 (12) (2001) 1813–1821.

[16] H. Schad, G. Baur, G. Meier, Investigation of the dielectric constants and the diamagnetic anisotropies of cyanobiphenyls (CB), cyanophenylcyclohexanes (PCH), and cyanocyclohexylcyclohexanes (CCH) in the nematic phase, J. Chem. Phys. 71 (8) (1979) 3174–3181.

[17] U. Finkenzeller, T. Geelhaar, G. Weber, L. Pohl, Liquid-crystalline reference compounds, Liq. Cryst. 5 (1) (1989) 313–321.

[18] M. Bender, P. Holstein, D. Geschke, Homogeneous and inhomogeneous director dynamics of a fluorinated liquid crystal, Mol. Cryst. Liq. Cryst. 363 (2001) 85–95.

[19] P. Holstein, M. Bender, Application of electric fields in NMR, Macromol. Symp. 184 (2002) 137–152.

[20] D.M. Brink, G.R. Satchler, Angular Momentum, Oxford University Press, London, 1968.

[21] M.E. Rose, Elementary Theory of Angular Momentum, Wiley, New York, 1967.